EUROPEAN FUSION DEVELOPMENT AGREEMENT

EFDA–JET–PR(03)16

L. Garzotti, X. Garbet, P. Mantica, V. Parail, M. Valovic, G. Corrigan,
D. Heading, T. T. C. Jones, P. Lang, H. Nordman, B. Pégourié, G. Saibene,
J. Spence, P. Strand, J. Weiland and JET EFDA contributors

Particle Transport and Density Profile Analysis of Different JET Plasmas

Particle Transport and Density Profile Analysis of Different JET Plasma

L. Garzotti[1], X. Garbet[2], P. Mantica[3], V. Parail[4], M. Valovic[4], G. Corrigan[4], D. Heading[4], T. T. C. Jones[4], P. Lang[5], H. Nordman[6], B. Pégourié[4], G. Saibene[7], J. Spence[4], P. Strand[6], J. Weiland[6]
and JET EFDA contributors*

[1]Consorzio RFX - Associazione EURATOM-ENEA sulla Fusione, I-35127 Padova, Italy
[2]Association EURATOM-CEA,CEA/DSM/DRFC,CEA-Cadarache,13108 St. Paul-lez-Durance, France
[3]Istituto di Fisica del Plasma EURATOM-ENEA-CNR association, Milan, Italy
[4]EURATOM-UKAEA Fusion Association, Culham Science Centre, OX14-3DB, Abingdon, UK
[5]Max Planck Institut für Plasmaphysik, IPP-EURATOM Assoziation, D-85748 Garching,Germany
[6]Association EURATOM-VR, Chalmers University of Technology, SE-41296 Göteborg, Sweden
[7]EFDA Close Support Unit Garching, c/o Max Planck Institut für Plasmaphysik, D-85748, Garching, Germany
** See annex of J. Pamela et al, "Overview of Recent JET Results and Future Perspectives", Fusion Energy 2000 (Proc. 18th Int. Conf. Sorrento, 2000), IAEA, Vienna (2001).*

Preprint of Paper to be submitted for publication in
Nuclear Fusion

ABSTRACT.
Over the last two years, several experiments, relevant for the study of particle transport and density profile evolution, have been performed on JET. They can be classified as stationary discharges with and without central particle source due to the beams, quasi-stationary discharges with deuterium gas puffing, deep pellet fuelled discharges and discharges perturbed by cold pulses obtained by shallow pellet injection. All these experimental scenarios have been simulated by means of the JETTO transport code, employing different transport models: purely empirical models, the semi-empirical mixed Bohm/gyro-Bohm transport model, both with the addition of different theory-based expression for the anomalous particle pinch and the first principle Weiland transport model. In this paper the results of the simulations are presented. The main conclusions are that, for the cases studied in this paper, the sawteeth activity is the main particle diffusion mechanism in the plasma centre ($r/a \leq 0.5$). Nevertheless, to reproduce the density profile in the gradient zone ($0.5 \leq r/a \leq 0.9$), an anomalous pinch seems to be necessary, at least for L-mode plasmas. This anomalous convective flux is well reproduced by the off-diagonal elements of the transport matrix given by the Weiland model.

1. INTRODUCTION

Particle transport and mechanisms leading to a given density profile are key issues to understand results from present experiments and to design next generation devices.

In particular the existence of an anomalous pinch velocity on top of the neo-classical Ware pinch has been the object of theoretical and experimental activity over the past years.

In some cases (like, for example, ASDEX-U) the analysis of the experimental results seems to indicate that the Ware pinch alone could be responsible for the observed peaking of the density profile [1]. On the other hand other experiments performed on Tore-Supra, featuring completely non-inductive plasma current and zero toroidal electric field and where, therefore, there is no Ware pinch, show a significant peaking of the density profile, which suggests that an anomalous pinch should be at work [2, 3]. Electron density profiles peaked inside the depth of the ionization source have been observed also on DIII-D, TCV and TEXTOR [4, 5]. An anomalous pinch velocity is predicted by theories describing transport induced by turbulence due to Ion Temperature Gradient (ITG) and Trapped Electron (TE) modes [6, 7, 8, 9].

In order to investigate this subject, a variety of shots, relevant for the study of particle transport and density profile evolution, performed on JET during the last experimental campaigns, has been selected in order to systematically cover a set of experimental scenarios as completely as possible. The JETTO transport code has been used with purely empirical, semi-empirical and physics-based diffusion models to analyze and simulate the selected discharges.

This paper presents the results of these simulations and compares them with experimentally determined profiles. The paper is organized as follows: a description of the different experimental scenarios simulated is given in section 2, in section 3 the models used in the simulation are described,

in section 4 the results of the simulations are presented, in section 5 there is a discussion of the modelling work and in section 6 conclusion are drawn.

2. DESCRIPTION OF THE SHOTS ANALYZED

The experimental scenarios analyzed are classified as follows:

- stationary, radio-frequency (RF) only heated discharges, without central particle source (beam fuelling),
- quasi-stationary or slowly evolving discharges with moderate gas puffing [10] and
- pellet fuelled discharges both strongly perturbed by deep pellet injection [11] and moderately perturbed by shallow pellet [12].

The discharges analyzed are summarized in table 1:

Table 1: Main parameters of the shots simulated

Pulse No:	B_T (T)	I (MA)	P_{NBI} (MW)	P_{ICRH} (MW)	n_{eo} (10^{19} m^{-3})	T_{eo} (keV)	T_{io} (keV)	Mode	ν^*
51034	2.3	2.3	–	4	1.5	6	2.3	L	0.03
49030	3.2	2.5	1	4.5	7	2	3.2	L	0.15
55804	3.4	1.6	–	3.5	2.9	3.5	3.4	L	0.07
51084	2.6	2.3	7.6	5	2.5	6.5	2.6	L	0.03
52961	2	1.9	8	–	7	3	2	H	0.25
52979	2	1.9	10.4	–	9	2.5	2	H	0.25
47744	2.7	2.1	1.2	10	5	5	2.7	H	0.05

Pulse No. 51034 is a stationary, RF only heated, low density, L-mode plasma. It is the simplest case to simulate because of the absence of uncertainties on the sources in the plasma core.

Pulse No: 49030 is a deep pellet fuelled, high density, L-mode plasma. The pellet injection frequency was 5 Hz whereas the LIDAR Thomson scattering sampling frequency was 4 Hz. This allows a reconstruction of the post-pellet density profile evolution with 50 ms time resolution. This is a scenario somewhat more complicated than that of shot 51034, because it is transient and there is the need to simulate the pellet effect.

Pulse No: 55804 is an L-mode plasma where a shallow pellet was injected to generate a cold pulse and study its propagation.

Pulse No: 51084 is also an L-mode plasma with shallow pellet injection, however in this case the target discharge was an optimized shear plasma, with a flatter q-profile than Pulse No: 55804 [12].

Pulse No: 52961 is a neutral beam heated, high density, sawtoothing, ELMy H-mode plasma. In this particular case the beam power was not high enough to maintain the sawteeth activity. Therefore the density profile remains stationary until the sawteeth are lost because of the relatively low beam power. Then the peaking of the density profile starts to increase due to the central beam particle source and finally the plasma disrupts. Deuterium puffing ($2.5 \bullet 10^{22}$ atom/s) was performed during the discharge.

Pulse No. 52979 is similar to Pulse No. 52961. The main difference is that, for this discharge, the beam power was high enough to sustain the sawteeth activity which controls the central density and prevents the density profile from peaking.

Pulse No. 47744 is a mainly RF heated, ELMy H-mode plasma. It can be considered on one side as the H-mode counterpart of Pulse No. 51034 and on the other side similar to Pulse No. 52979, where most of the NBI heating power has been replaced by ICRH.

3. DESCRIPTION OF THE MODELS USED

The discharges described in the previous section have been simulated by means of the JETTO transport code. Three kind of transport models have been tested: purely empirical transport models, the semi-empirical mixed Bohm/gyro-Bohm transport model [13] and the first principle Weiland's model [14], based essentially on transport induced by ITG and trapped electron modes.

In the purely empirical simulation the diffusion coefficient profiles are prescribed using the analytical formula:

$$D(\rho) = (D_0 - D_\alpha)(1 - \rho^{\alpha_D}) + D_\alpha$$

where D_0 and D_α are the centre and edge value of the diffusion coefficient and ρ is the normalized radius.

In the mixed Bohm/gyro-Bohm transport model, the electron and ion thermal conductivity are linear combination of a Bohm like and a gyro-Bohm like term:

$$\chi_{e,i} = \chi^B_{e,i} + \chi^{gB}_{e,i}$$

$$\chi^{gB}_e = \alpha_B \frac{cT_e}{eB_t} L^{*-1}_{pe} q^2; \quad L^*_{pe} = \frac{p_e}{a|\nabla p_e|}; \qquad \chi^B_i = 2\chi^B_e$$

$$\chi^{gB}_e = \alpha_{gB} \frac{cT_e}{eB_t} L^{*-1}_{Te} \rho^*; \quad \rho^* = \frac{M^{1/2} c T_e^{1/2}}{Z_i e B_t}; \quad \chi^{gB}_i = \chi^{gB}_e$$

$$\alpha_B = 8 \times 10^{-5} \qquad \alpha_{gB} = 3.5 \times 10^{-2}$$

the particle diffusion coefficient is obtained as:

$$D = S \frac{\chi_e \chi_i}{\chi_e + \chi_i}$$

where $S(r)$ is a weight function such as $S(0) = 1.0$ and $S(a) = 0.3$.

As already said particular attention was paid to the effect of an anomalous particle pinch velocity V. Both in the purely empirical and in the mixed Bohm/gyro-Bohm models this was introduced according to the expressions:

$$V = c_T D \nabla T/T ; \qquad V = -c_q D \nabla q/q.$$

It is worth noting that when the total flux is written as $\Gamma = -D\nabla n + Vn$, a negative V corresponds to an inward pinch.

The justification for using such expressions comes from the evaluation of the radial particle flux due to ITG and TE modes [6, 7] which predicts convective terms proportional to D and $\nabla T/T$ or $\nabla q/q$. A different theory known as turbulence equipartition [8], based on the conservation of the product $n(r)q(r)$ along the plasma minor radius, also implies that a convective term proportional to $\nabla q/q$ should appear in the particle flux.

In the version of the Weiland model employed in this study passing electron are considered adiabatic. Equations are solved for the trapped electron temperature and for the main and impurity ion density and temperature. A further equation for the parallel component of the vector potential A k takes into account electromagnetic effects. The growth rates of the ITG and TE modes are calculated for each point of the radial mesh. Then the transport is summed over the unstable modes and an estimate of the saturated amplitude of the modes is used to build the transport matrix [14, 15].

Here the convective particle flux is introduced in the code by the presence of off-diagonal elements in the transport matrix, containing terms depending on $\nabla n/n$, $\nabla T/T$ and $\nabla B/B$.

In all cases, whenever the energy sources were available, complete simulations have been performed for electron density and electron and ion temperature. However the analysis of the density behaviour has been emphasized and the agreement between simulated and measured density profiles has been optimized. Nevertheless the reproduction of the temperature behaviour is also satisfactory, although a systematic tendency to underestimate the central temperature for the mixed Bohm/gyro-Bohm model and of overestimate it for the Weiland model is observed. On the other hand simulations have been done for the density alone prescribing the experimental behaviour of both electron and ion temperature, when available, and the results did not show substantial differences when compared with the cases when both density and temperature were simulated.

As to impurities, they are treated in JETTO interpretatively. In fact, the experimental Z_{eff} profile and dominant impurity species are specified and used throughout the simulation.

4. SIMULATION RESULTS

As the results show some differences the analysis of the L-mode is presented first, whereas the simulations of the H-mode plasmas are described separately.

4.1. L-MODE

Figure 1 illustrates the results of the simulations for shot 51034. Since the density profile was stationary over the simulated time interval, the time-averaged density profiles are shown. It can be seen that both the mixed Bohm/gyro-Bohm and the Weiland model reproduce reasonably well the shape of the density profile. In order to simulate the central density behaviour, however, it has been necessary to introduce in the mixed Bohm/gyro-Bohm model an anomalous pinch velocity, which can be 5 to 15 times larger than the neo-classical Ware pinch. As already said this velocity has been

modelled by two theory based expressions, $V = c_T D\nabla T/T$ and $V = -c_q D\nabla q/q$. In this case the values of c_T and c_q used in the simulation were 0.25 and 0.75 respectively. Finally, in order to assess the weight of the off-diagonal elements in the Weiland's model, a simulation was performed after dropping them from the transport matrix. In this case the agreement with the experimental measurements was poorer and a result similar to that obtained with the mixed Bohm/gyro-Bohm model without anomalous pinch was obtained.

In can be noted that even in presence of the Ware pinch alone (which is of the order of 10^{-2} m/s) the profiles are not completely flat. This is due partly to the Ware pinch itself (which is responsible for the modest peaking inside $r/a \leq 0.6$) and partly to the relatively deep penetration of the neutrals in low density shots like the one analyzed (which accounts for the peaking in the outer part of the plasma). However, the peaking of the profiles obtained with an anomalous pinch cannot be justified simply by the uncertainty in the neutral penetration. To show it, different simulations have been performed varying only the energy of the incoming neutrals. The results are shown in figure 2 and show that a variation of an order of magnitude in this parameter does not affect dramatically the shape of the density profile.

Figures 3 and 4 show the results of the simulations for Pulse No. 49030. Since the density profile was changing during the simulated time interval, the time evolution of the density profile is shown rather than their average shape.

It can be seen, from experimental data, that, for this shot, the volume average density after pellet injection decreases to the pre-pellet value on a time scale of 200ms. The complete relaxation of the pellet deposition profile takes place in about 100-150ms. The central density ne(0) is more noisy, but it can be estimated that it increases for the first 500ms after the start of the pellet sequence, before reaching an essentially stationary value.

As for Pulse No. 51034, the mixed Bohm/gyro-Bohm model with the addition of an anomalous pinch velocity gives results compatible with the experimental evolution of the volume average density and of the density profile. The pinch velocity has been modelled in the same way as for shot 51034 and can be up to one order of magnitude greater than the neo-classical Ware pinch. In this case c_T and c_q used in the simulation were 0.125 and 0.25 [16] respectively. Similar results are obtained with the Weiland model.

It is worth nothing, however, that both models predict an inward propagation and a relaxation of the pellet density perturbation slightly faster than that observed experimentally. This may indicate at least that either the profiles of the particle diffusion coefficient provided by the models are not completely adequate to describe all the details of the post-pellet density evolution or the hypothesis of c_T and c_q constant in time is too strong and has to be relaxed. This will be the object of future investigation.

Figures 5 and 6 show the results for the first case with shallow pellet injection. In figure 5 the simulated values of volume average and on-axis density for different runs are plotted and compared with the LIDAR Thomson scattering experimental measurements [17]. It is interesting to note that,

experimentally, the increase in the on-axis density is seen to last for the 100-250 ms after the pellet injection. To complement this information, in figure 6 the simulated density line integrals along a centre and an edge chord are presented for the same runs and compared with the experimental values measured by the interferometer.

Here the purely empirical transport model has been used with $D_0 = D_a = 0.3$ m^2/s, in order to reproduce at the same time the evolution of the volume average density and of the line integral density along the interferometer chords.

The simulation is in line with the previous results, that is the analytical model reproduces the experimental observations provided that an anomalous pinch is added.

In this case values of $c_T = 0.25$ and $c_q = 0.5$ have been used.
On the other hand no pinch is needed to simulate the optimized shear case (in fact the simulation overestimates the density peaking even without any pinch as shown in figures 7 and 8). Also, in this case, careful inspection of the experimental data provided by the LIDAR, the interferometer and the electron cyclotron emission radiometer shows no evident effect of the pellet on the on-axis density and temperature.

This indicates that two, possibly synergetic, phenomena may be occurring: as an effect of the optimized shear, turbulence is quenched and D is lower than in other L-mode plasmas, moreover, because of the different current profile, ∇q is smaller in an optimized shear plasma. Both effects contribute to reduce the importance of a pinch velocity proportional to $D\nabla q/q$. Although it is not easy to identify the actual relative weight of the two phenomena, these experimental and simulation results seem to point toward a pinch of the kind $V = -c_q D\nabla q/q$ rather than $V = c_T D\nabla T/T$. To estimate the error bars on c_T and c_q the following quantity has been considered [16, 18]:

$$\Delta^2 = \frac{\Sigma_{j=1}^{N} [(n_{exp}(x_j) - n(x_j)) / n(x_j) - m]^2}{N}$$

$$m = \frac{\Sigma_{j=1}^{N} [(n_{exp}(x_j) - n(x_j))/n(x_j)]}{N}$$

Using LIDAR profiles and error bars, values of $\Delta \approx 5\%$ are obtained. Similar values are obtained when both c_T and c_q are varied by 0.1 from one simulation to another. A confidence interval of ± 0.1 has therefore been assumed on both these parameters.

4.2. H-MODE

Simulation results for Pulse No: 52961 are presented in figures 9 and 10. As before, since the density is slowly evolving in time the time evolution of the profiles is shown. It can be seen that, for this kind of plasmas, the Weiland's model gives good agreement with the experimental profiles, particularly in the gradient zone ($0.5 \leq r/a \leq 0.9$), whereas the mixed Bohm/gyro-Bohm model tends to produce a more box-shaped profile. The anomalous pinch velocity has been introduced in the mixed Bohm/gyro-Bohm model in the same way as in the L-mode discharges previously analyzed.

However, in this case, the pinch velocity is one order of magnitude smaller than in the L-mode plasma and is comparable with the Ware pinch. Therefore the results of the simulations do not depend dramatically on whether an anomalous pinch is taken into account or not. This is a consequence of the fact that V is proportional to D and that, in H-mode, the particle diffusion coefficient is almost an order of magnitude smaller than in L-mode. A final comment can be made on the balance between the flattening of the density profile due to the sawteeth activity and the particle source due to the beams. It can be seen that the sawteeth are responsible for the flattening of the density profile in the plasma centre (for the shots analyzed here the mixing radius was r/a ≈0.5) and that, when they are switched off at t = 61:75 s in the simulation to reproduce the experimental behaviour, the beam source alone can account for the central density increase.

The results of the simulations for Pulse No: 52979 are shown in figure 11. Time averaged profiles are shown because, as for Pulse No: 51034, the plasma was stationary over the simulated time interval. The same remarks done for Pulse No: 52961 apply: the Weiland model better reproduces the experimental density than the mixed Bohm/gyro-Bohm model and the anomalous pinch velocity is reduced by one order of magnitude becoming comparable to the Ware pinch. As for the sawteeth, they are present throughout the entire simulated time interval and their effect is to maintain a constant central density and prevent the profile peaking due to the beam particle source.

To conclude and complete the analysis Pulse No: 47744 (H-mode mainly RF-heated) has been simulated and the results are shown in figure 12. On one side it is confirmed that the mixed Bohm/gyro-Bohm model does not need a significant pinch velocity to reproduce the experimental profile, enforcing the conclusion that an anomalous pinch velocity is not evident in H-mode. On the other hand, when the Weiland model is applied to this Pulse No:, it fails in reproducing the observed density profile, giving an overestimate of the central density value and of the overall density peaking.

The reason for this behaviour is still unclear and will be the object of future investigation. However some differences in parameters relevant for ITG and TE stability and which could be responsible for this results can be noticed. Beside the heating scheme, which can modify the ratio pi=pe between power deposited in the ion and electron channels respectively, Z_{eff} is different between the two kinds of Pulse No's, being ≈1.5 for Pulse No's: 52961 and 52979 and ≈ 2.5 for Pulse No. 47744 and collisionality is also a factor of 5 larger in Pulse No's 52961 and 52979 than in Pulse No. 47744.

SUMMARY AND DISCUSSION

From the results presented in the previous section the following picture emerges: an anomalous pinch velocity is needed to reproduce the behaviour of the density profiles in the shots considered. Being the pinch proportional to D its effect is evident in L-mode plasmas where the confinement can be an order of magnitude lower than in H-mode.

The results for the L-mode simulations are summarized in table 2 where the values of c_T and c_q employed in the simulations are reported together with the ability of the full Weiland model (i. e. with all the off-diagonal elements of the transport matrix) to reproduce the experimental profiles.

Pulse No:	Anomalous pinch		Weiland
	c_T	c_T	
51034	0.25	0.75	yes
49030	0.125	0.25	yes
55804	0.25	0.5	yes
51084	–	–	No

Table 2: Summary of the simulation results for L-mode plasmas

It can be noted that the values of c_T and c_q vary from case to case. Plotting both c_T and c_q as a function of ν^* (see figure 13), it can be argued that the values of c_T and c_q, and therefore the effect of the anomalous pinch, tend to increase at low collisionality, in qualitative agreement with what has recently been found in ASDEX upgrade [20]. This would suggest that the stabilizing effect of collisions on TE modes reduces the effect of the anomalous pinch.

The analysis of the H-mode plasmas seems to confirm the trend identified in L-mode, at least as far as NBI heated plasmas are concerned. Both the mixed Bohm/gyro-Bohm model with no or little pinch velocity and the Weiland model reproduce the experimental results. In H-mode however the anomalous pinch is of the order of the neo-classical Ware pinch because turbulence is reduced and the diffusion coefficients are smaller than in L-mode. There are however exceptions when mainly RF-heated discharges are taken into account. In this case the mixed Bohm/gyro-Bohm model continues to work, but the Weiland model breaks down and gives too peaked density profiles. It is unlikely that the sawteeth activity is responsible for the difference because it was similar in all the H-mode plasmas analyzed. Likewise collisions are not a strong candidate to explain this discrepancy, because, if they were, the effect of the pinch due to TE modes should be larger at low collisionality. Instead the shot with lower ν^* (47744) shows flatter density profiles than the other two (52961 and 52979). A role might be played by both Z_{eff} and the ratio p_i/p_e, which are different in the two kinds of shot analyzed, but a clear answer is still missing insofar and this point will be the subject of future analysis.

CONCLUSIONS

Particle transport and density profile behaviour have been simulated for different JET plasmas with the JETTO code using the mixed Bohm/gyro-Bohm and the Weiland transport model. The main conclusions regard in general the particle diffusion mechanisms at work and in particular the existence of an anomalous convective particle flux.

In the plasma centre ($r/a \leq 0.5$) the sawteeth activity is the main particle diffusion mechanism. In the gradient region ($0.5 \leq r/a \leq 0.9$) the Weiland model simulates the density profiles better than the mixed Bohm/gyro-Bohm model. Moreover, in this region, an anomalous pinch proportional to $\nabla q/q$ in the Bohm/gyro-Bohm model is necessary to reproduce the experimental observations. This anomalous convective flux, being proportional to D, is evident in L-mode plasmas and reduces to

the neo-classical level for H-mode plasmas. In almost all the shots considered, the off-diagonal elements of the transport matrix in the Weiland model provide the convective flux adequate to reproduce the observed density profile peaking.

ACKNOWLEDGEMENTS

This work has been performed under the European Fusion Development Agreement. We would like to thank Dr. Clemente Angioni for useful comments and discussion.

REFERENCES

[1]. Stober J, Gruber O, Kaufmann M, Neu R, Ryter F, Sandmann W, Zohm H and the ASDEX Upgrade Team 2000 Plasma Phys. Control. Fusion **44** A159

[2]. Tore Supra Team 2002 19th IAEA Fusion Energy Conference Lyon, France, 14-19 Oct. 2002

[3]. Hoang G T et al., submitted to Phys. Rev. Lett.

[4]. Weisen H and Minardi E 2001 Europhys. Lett. **56** 542

[5]. Tokar M Z, Ongena J, Unterberg B and Weynants R R 2000 Phys. Rev. Lett. **84** 895

[6]. Baker D R and Rosenbluth M N 1998 Phys. Plasmas **5** 2936

[7]. Dominguez R R 1993 Phys. Fluids B **5** 1782

[8]. Yankov V V and Nycander J 1997 Phys. Plasmas **4** 2907

[9]. Garbet X et al., submitted to Phys Rev. Lett.

[10]. Valovic M, Rapp J, Cordey J C, Budny B, McDonald D C, Garzotti L, Kallenbach A, Mahdavi M A, Ongena J, Parail V, Saibene G, Sartori R, Stamp M, Sauter O, Strachan J, Suttrop W and contributors to the EFDA-JET Workprogramme 2002 Plasma Phys. Control. Fusion **44** 1911

[11]. Jones T T C, Baylor L R, Challis C D, Cox S J, Gormezano C, Gowers C W, Horton L D, Lang P T, Lomas P J, Matthews G F, Saibene G, Twynam P, Walden A D, Watson M J, Wijetunge S and Willis B L 2000 in Controlled Fusion and Plasma Physics (Proc. 27th Eur. Conf. Budapest, 2000 Vol. 24B (Mulhouse: European Physical Society) 13

[12]. Mantica P, Gorini G, Imbeaux F, Kinsey J, Sarazin Y, Budny R, Coffey I, Dux R, Garbet X, Garzotti L, Ingesson C, Kissick M, Parail V, Sozzi C, Walden A and contributors to the EFDA-JET Workprogramme 2002 Plasma Phys. Control. Fusion **44** 2185

[13]. Erba M, Cherubini A, Parail V V, Springmann E and Taroni A 1997 Plasma Phys. Control. Fusion **39** 261.

[14] Weiland J 2000 Collective Modes in Inhomogeneous Plasma - Kinetic and Advanced Fluid Theory (Bristol and Philadelphia: Institute of Physics Publishing)

[15]. Strand P, Nordman H, Weiland J and Christiansen J P 1998 Nucl. Fusion **38** 545

[16]. Garzotti L, Corrigan G, Heading D, Jones T T C, Parail V, Pégourié B, and Spence J 2000 in Controlled Fusion and Plasma Physics (Proc. 27th Eur. Conf. Budapest, 2000 Vol. 24B (Mulhouse: European Physical Society) 316

[17]. Gowers C W, Brown B W, Fajemirokun H, Nielsen P, Nizienko Y and Schunke B 1995 Rev. Sci. Instrum. 66 471
[18]. Erba M, Parail V, Springmann E, Taroni A 1995 JET Report JET-R(95)02
[19]. Nillson J and Weiland J 1994 Nucl. Fusion **34** 803
[20]. Angioni C et al., submitted to Phys. Rev. Lett.

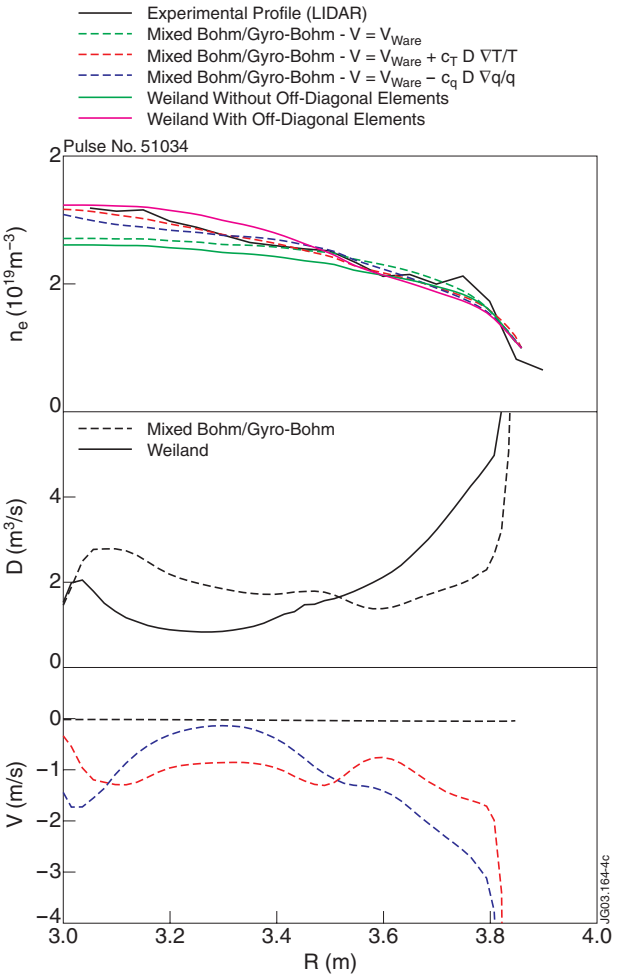

Figure 1: Simulation results for Pulse No.51034. In the top frame are plotted the time averaged density profiles. The simulated time interval goes from 5.13 s to 7.88s. As explained in the legend, the black solid line is the experimental profile. The dashed lines are the simulations obtained with the mixed Bohm/gyro-Bohm transport model without pinch (green), with $V = c_T D\nabla T/T$ and $c_T = 0.25$ (red) and with $V = -c_q D\nabla q/q$ and $c_q = 0.75$ (blue). The coloured solid lines are the results of the Weiland model with (magenta) and without (green) taking into account the off-diagonal elements of the transport matrix. The second frame shows the particle diffusion coefficient given by the mixed Bohm/gyro-Bohm model (dashed line) and the effective particle diffusion coefficient given by the Weiland model (solid line). The bottom frame shows the Ware, $\nabla T/T$ and $\nabla q/q$ pinch velocities (black, red and blue dashed lines respectively). These line and colour convention will be maintained throughout the rest of the paper.

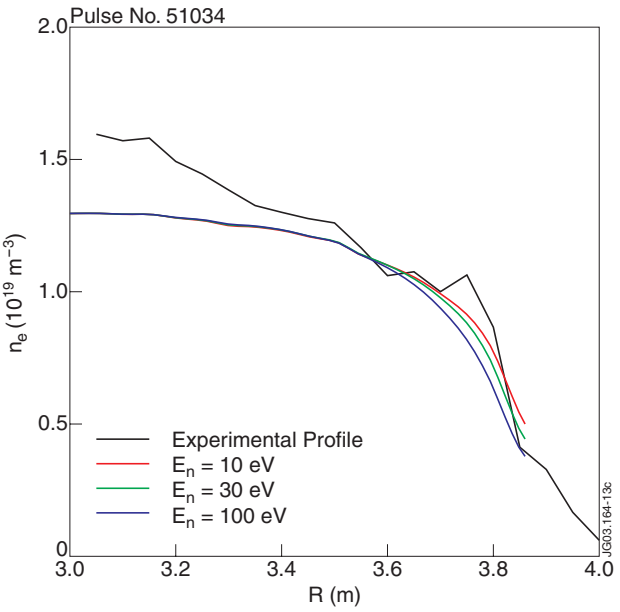

Figure 2: Effect of the energy of the recycling neutrals on the peaking of the density profile.

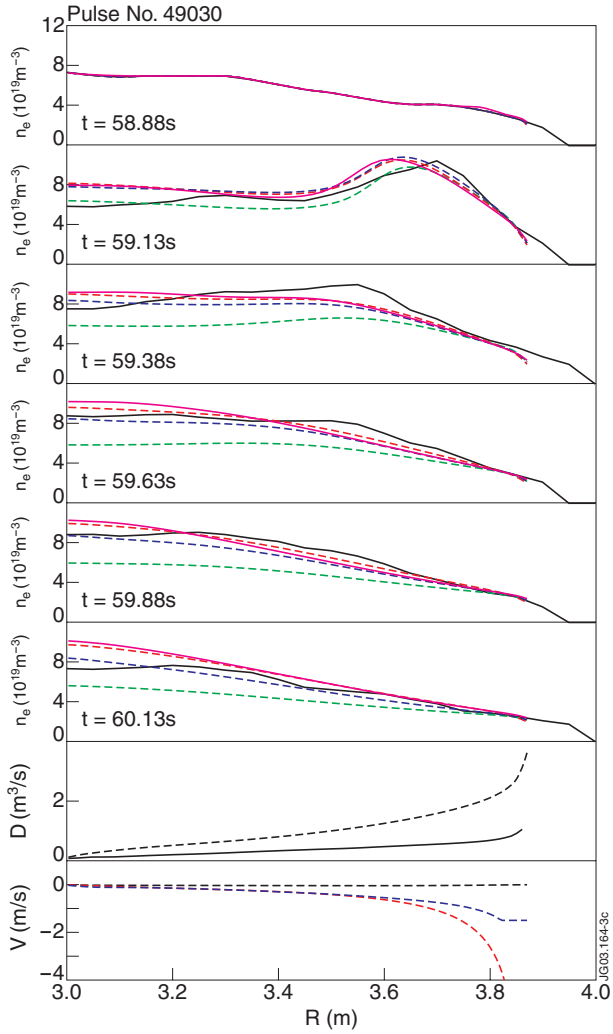

Figure 3. Simulation results for Pulse No. 49030. The first six frames show the density profile evolution. The seventh frame shows the particle diffusion coefficient given by the mixed Bohm/gyro-Bohm model and the effective particle diffusion coefficient given by the Weiland model. The last frame shows the Ware, ∇T/T and ∇q/q pinch velocities. The meaning of the colours and linestyles is the same as in figure 1.

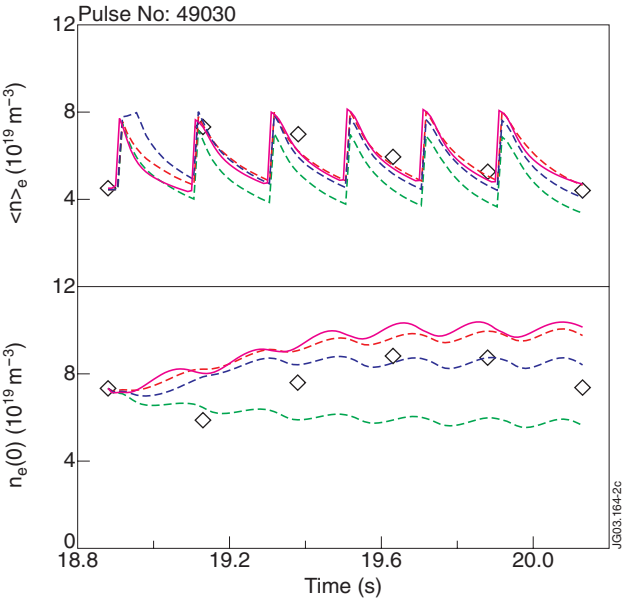

Figure 4. Density time traces for the simulations of Pulse No. 49030. The meaning of the colours and linestyles is the same as in figure 1. The open diamonds are the experimental LIDAR measurements. The top frame shows the evolution of the volume average density whereas the bottom frame shows the evolution of the on axis density.

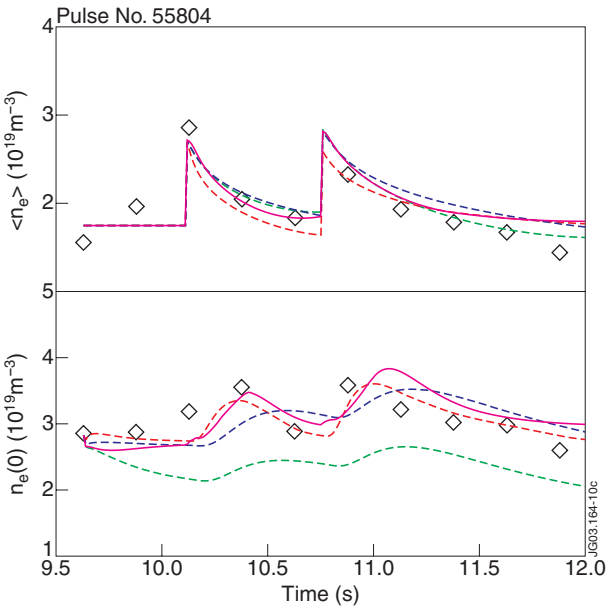

Figure 5. Same as figure 4 for Pulse No. 55804. In this case the dashed lines correspond to the results of the purely empirical model described in the text.

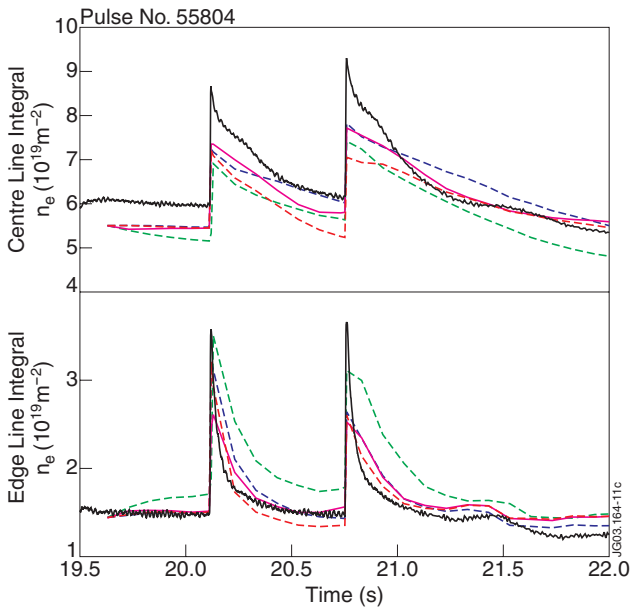

Figure 6. Density line integral along a centre and edge line of sight of the JET interferometer for Pulse No: 55804.

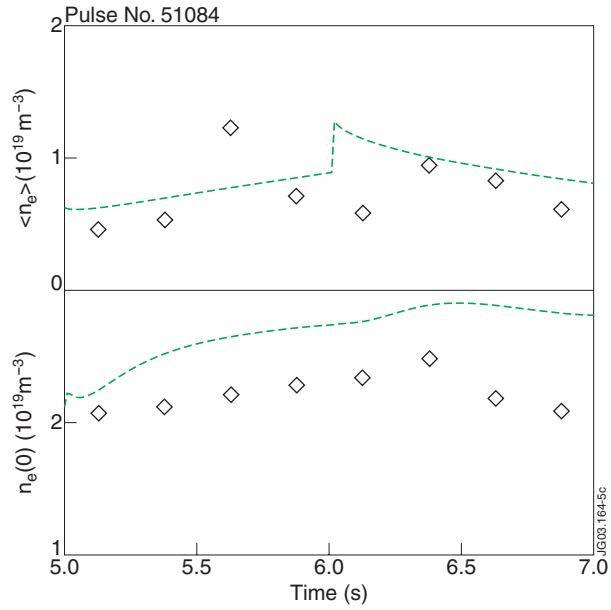

Figure 7: Same as figure 5 for Pulse No. 51084.

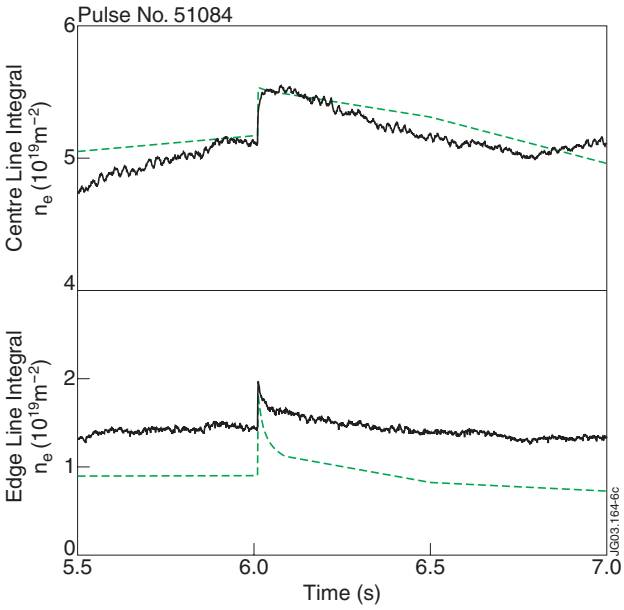

Figure 8: Same as figure 6 for Pulse No. 51084.

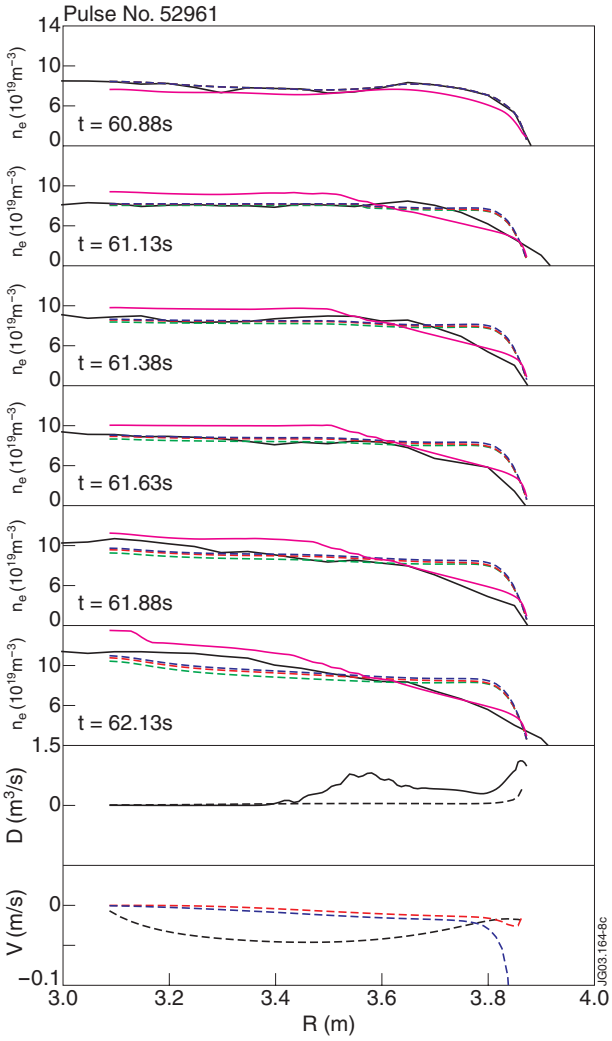

Figure 9: Same as figure 3 for Pulse No: 52961.

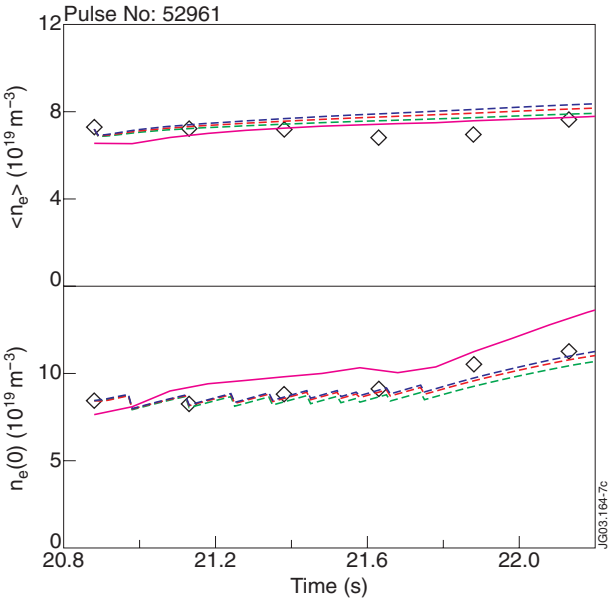

Figure 10: Same as figure 4 for Pulse No: 52961

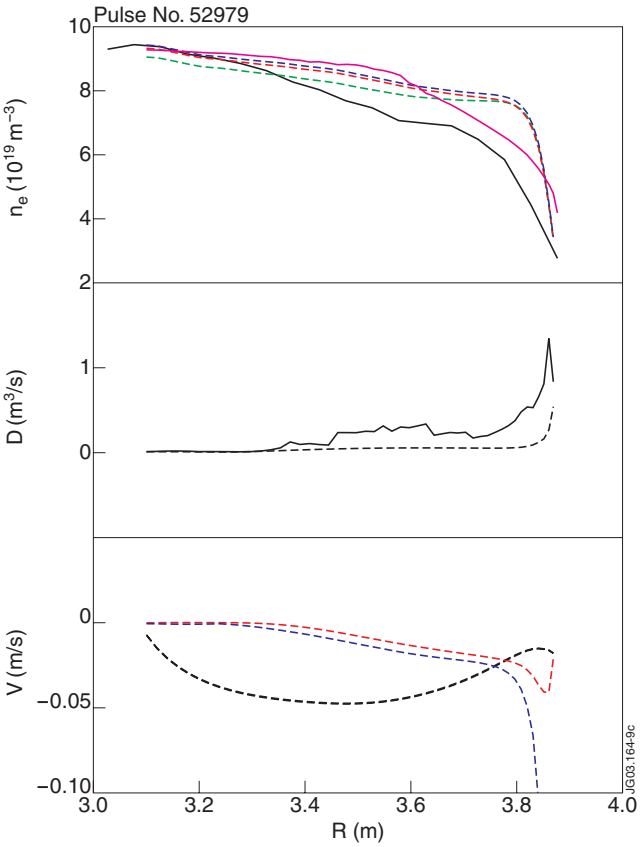

Figure 11: Same as figure 1 for Pulse No: 52979. The simulated time interval goes from 22.88s to 23.88s.

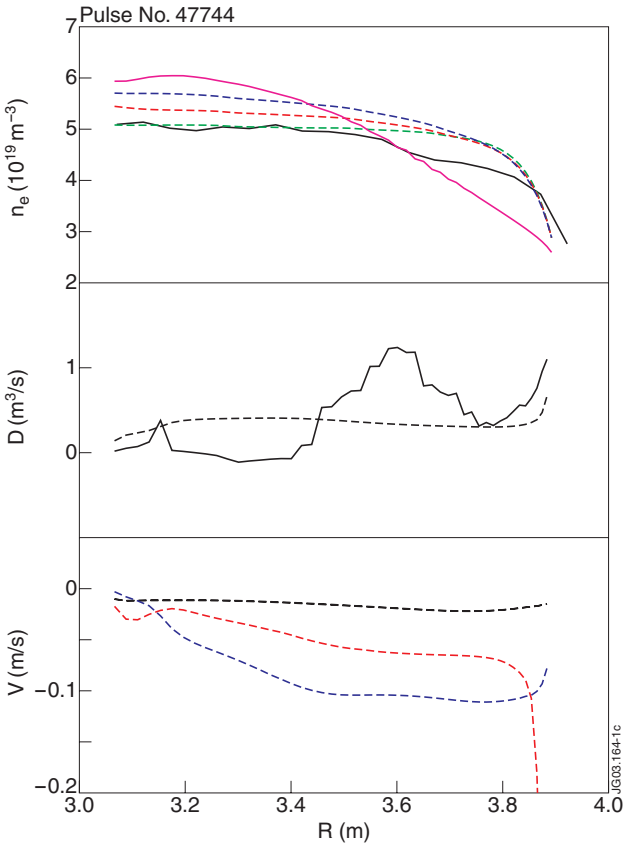

Figure 12. Same as figure 1 for Pulse No: 47744. The simulated time interval goes from 20.88s to 24.13s.

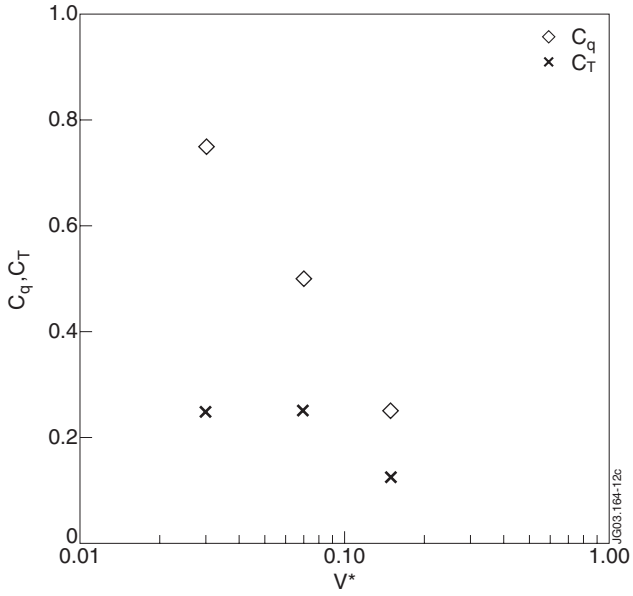

Figure 13. Dependence of the coefficients c_T and c_q on the dimensionless collisionality ν^*.